

## Mobile Phone Radiation Induced Plasma Protein Alterations And Eye Pathology In Newly Born Mice

F. Eid\*, M. Abou Zeid \*\*, N Hanafi \*\*\* and A. El-Dahshan\*

\*Zoology Department, Faculty of Science for Girls, Al-Azhar University, Cairo, Egypt. \*\*Zoology Department, Faculty of Science, Al-Azhar University, Cairo, Egypt.

\*\*\* Radiation Biology Department, National Centre for Radiation Research and Technology (NCRRT), Atomic Energy Authority (AEA), Cairo, Egypt.

**Abstract:** The hazardous health effect of the exposure to 900-1800 MHz radiofrequency electromagnetic fields (RF-EMF) which emitted from mobile phones was investigated on the plasma protein and eye of newly born mice. Twenty one newly born mice were divided into 3 groups, the 1<sup>st</sup> group served as control, the 2<sup>nd</sup> group exposed to mobile phone radiation daily for one month (45 min/day) and the 3<sup>rd</sup> group remained one month following the end of exposure. The results showed deleterious changes in the plasma protein pattern by electrophoretic analysis. Also, the microscopic examination demonstrated numerous histopathological and histochemical changes in the eye mainly represented by degenerated, hemorrhagic areas and detachment in some layers of the eye with alteration in collagen, polysaccharides, total protein and marked increase in amyloid beta ( $\beta$ ) protein contents of newly born mice exposed to RF-EMF from mobile phone (45 min/day) for one month as well as after one month following the end of exposure. It was concluded that the exposure to mobile phone radiation causes plasma proteins alterations and eye pathology in newly born mice.

### Introduction

The field of mobile communications is rapidly developing and mobile technology has a high rate of adoption in the daily life of the population. All layers of the population use mobile phones. Mobile phones emit RF-EMF and impulse magnetic fields (MF) during calls. This RF-EMF can penetrate 4-6 cm into the human brain [1, 2]. RF-EMF are transmitted and received in the range 400–2000 megahertz (MHz). However, the cellular target of RF-EMF is still controversial, several recent studies have indicated that RF-EMF have an adverse effect on most organs of mice especially on newly born mice.

There are many effects of EMFs on human such as cancer, epidemiology, acute and chronic effects. These effects vary according to the field strength and environmental conditions [3]. Modern children are exposed to RF fields from mobile phone for longer periods than adults, because they started using mobile phones at an early age and are likely to continue using those [4]. Kabuto *et al.* [5] confirmed that high EMF exposure in children's bedrooms was associated with a significantly higher risk of childhood leukemia. On the other hand, children exposed had less developed memory and attention, their reaction time was slower and their

neuromuscular apparatus endurance was decreased [6].

Challis [7] demonstrated that possible RF-EMF interactions include changes in the conformation of proteins, resulting in functional changes in these proteins. Also, Krstic *et al.* [8] reported that EM radiation caused increase in the levels of protein structural alteration, this increase led to significant disorders of function and structure of some cells in mice. The results of Lixia *et al.* [9] indicated that exposure to 1.8 GHz RF field of GSM can increase heat shock protein expression in human lens epithelial cells without change in the cell proliferation rate. The results of Karinen *et al.* [10] suggested that protein expression in human skin might be affected by the exposure to RF EMFs. Sypniewska *et al.* [11] concluded that the plasma of 35 GHz millimeter waves exposed rats increased the expression of 11 proteins. These altered proteins are associated with inflammation, and oxidative stress. The long-term irradiation to EMF from mobile phone altered significantly the expression of 143 proteins in mice such as neural function related proteins, heat shock proteins and the brain metabolism proteins [12]. A study from Germany reported a significant four-fold increased risk of malignant melanoma

of the eye associated with the use of RF transmitting devices, including mobile telephones [13]. Also, **Balik *et al.*** [14] found that mobile phone may cause blurring of vision, inflammation, secretion and lacrimation of the eyes. They observed also that mobile phone cause derangement of retinal differentiation in animal. **Balci *et al.*** [15] reported that the mobile phone effect on the oxidant/antioxidant balance in corneal and lens tissues of female albino Wistar rats. In addition, a study carried out by **Kucer** [16], using of mobile phones caused blurring of vision, redness of the eyes, vision disturbance, secretion of the eyes and inflammation in the eyes of users of mobile phones (women or men). 1800 MHz mobile phone radiation increased intracellular reactive oxygen species and DNA damage of lens epithelial cells [17]. **Nassar *et al.*** [18] found that 900- 1800 MHz non-ionizing radiation of the mobile phone has a marked degenerative effect on the retina of developing albino mice at the ultra structural level. They added that all the retinal layers exhibited a reduction in their height and cell population. **Khalil *et al.*** [19] observed that 900 MHz mobile phone like RF radiation caused noticeable differences between photoreceptors of retina of the control and exposed mice as bleaching of photoreceptors in the exposed mice. The purpose of the present work was to evaluate the effect of RF-EMF emitted from mobile phone on plasma proteins and eye layers of newly born mice.

## Material and methods

### Experimental design

Twenty one newly born Swiss albino mice (one day old) were maintained under controlled conditions of temperature (20-25°C) and light (12 hours light, 12 hours dark). They were divided into three equal groups. The 1<sup>st</sup> group served as the control, they were anesthetized and sacrificed after one month of the experiment, the 2<sup>nd</sup> group were exposed to RF-EMF from mobile phone (45min/day) for one month (exposed group, G<sub>1</sub>). At the end of the last exposure, mice were anesthetized and sacrificed and the 3<sup>rd</sup> group served as recovery group (G<sub>2</sub>), where newly born mice were exposed to RF- EMF as the 2<sup>nd</sup> group and then anesthetized and sacrificed after one month following the end of

exposure. Each group was caged in especially designed plastic container suitable for their size to permit good ventilation and free motion. Mice were fed on mother's milk until weaning then they were fed on bread, vegetables and standard rodent pellet diet with vitamins, minerals and freely supplied with drinking tap water. Meanwhile, the amount of used food was similar in each group.

### The exposure setup

Exposure of animals was performed by using a mobile phone radiation (Nokia, model 1280) at a specific absorption rate (SAR) of 0.78 W/Kg and frequencies from 900 to 1800 MHz at intensity 500µW/cm<sup>2</sup>, in connection with Egypt network (Vodafone, Egypt). The mice were exposed from the postnatal life and continue for one month. The exposure was performed as a daily repeated series (45 mints/ day). The mobile phone set on dialing mode and placed in a direct contact to the bottom of the exposure cage.

### Collection of blood samples

All animals were anaesthetized with chloroform inhalation. The blood samples were collected from the heart by heparinized syringes, and then transferred to heparinized vials. Plasma was obtained from the blood by centrifugation at 3000 rpm for 30 min. and kept in a deep freezer at -20°C till assayed for electrophoretic analysis.

### Electrophoretic analysis

The samples of mice plasma of all the experimental groups were separated using sodium dodecyl sulfate polyacrylamide gel electrophoresis, (SDS-PAGE).

### Histological and histochemical techniques

The eye tissue was collected from each group, dissected and processed for light microscope examination. Specimens for light microscope examination were fixed in 10% neutral buffered formol solution and Carnoy's fluid for the histological and histochemical studies. They were processed to prepare 5 µm thick paraffin sections and stained with Harris haematoxylin and eosin [20]. Collagen was detected by Mallory's trichrome stain [21]. Polysaccharides were detected by PAS (periodic acid Schiff) method [22]. Proteins were detected by mercuric

bromophenol blue method [23]. Amyloid  $\beta$  was detected by Congo red technique [24, 25].

#### Apoptosis and necrosis analysis

Apoptosis and necrosis were stained and analyzed using the method of Ribble *et al.* [26]. A mixture of acridine orange and ethidium bromide was prepared in PBS. The tissue uptake of the stain was monitored under a fluorescence microscope.

#### Image analysis

Image analysis software (Image pro-plus Ver. 5) was used in analysing the images which were obtained by the digital camera according to the method of Reedy and Kamboj [27]. The results were expressed as mean  $\pm$  standard deviation (SD) and were considered significant at the 5%.

#### Statistical analysis

The data were analyzed statistically according to Primer, statistica method (Ver. 5) which was described by Clarke and Gorley [28] to perform the different tests and illustrate the similarity percentages of collected data between the experimental animals.

#### Laboratory facilities

Facilities including animal housing and irradiation process had been made available by the National Center for Radiation Research and Technology (NCRRT). Electrophoretic analysis, histological, histochemical and quantitative image analysis was performed in the Department of Marine Biology, Faculty of Science, AL-Azhar University.

#### Results

The results of the present study showed deleterious changes in the plasma protein with numerous histopathological and histochemical changes in the eye of newly born mice exposed to RF-EMF from mobile phone radiation 45 min/day for one month as well as after one month following the end of exposure.

#### Plasma proteins separation with SDS-PAGE

Electrophoretic protein pattern of control newly born mice plasma:

The electrophoretic separation of plasma protein pattern of the normal control newly born mice

was done using SDS-PAGE gel as shown in table (1) and figure (1).

Scanning of the SDS-PAGE gel of the control newly born mice plasma proteins revealed the presence of clearly seen 14 visible protein bands, the molecular weight (MW) ranged from 168.21 to 9.432 kDa. There were seven bands of proteins with high molecular weight and other seven bands with low molecular weight. These bands were classified into 7 protein regions according to their molecular weight (Table 1&figure 1). List of probable protein regions is shown in table (1) as follows:

Region I: a single band with MW 168.21 kDa representing  $\alpha_1$ -lipoprotein,  $\alpha_2$ macroglobulins and  $\gamma$ -globulins.

Region II: represents the iron-transport protein, transferrin which migrated as 2 bands with MW 79.343 and 75.403 kDa.

Region III: comprise the albumin, prealbumin, prothrombin and antithrombin fractions which are considered as the most prominent proteins in the normal plasma. They were separated as a single band of MW 56.8 kDa.

Region IV: represents the largest band of MW 44.815 kDa which corresponded to  $\alpha_1$ -antitrypsin and  $\beta_2$ -glycoprotein I.

Region V: this region reveals one protein fraction of approximately MW 40.667 representing  $\alpha_1$ -acid glycoproteins.

Region VI: this fraction is represented by a single band of MW 36.519 kDa which was identified as  $\beta_2$ -Glycoprotein III.

Region VII: includes low molecular weight proteins which is separated as 7 protein fractions with approximately MW 30.593, 28.645, 24.806, 20.871, 9.432, 12.946 and 18.548 kDa.

Electrophoretic protein pattern of the exposed group ( $G_1$ ) of newly born mice plasma:

The electrophoretic analysis of plasma from  $G_1$  group exhibited lots of changes in the protein pattern as shown in table (1) and figure (2) which reveals a different pattern from that of the control group. This group included 12 bands, in comparison with 14 bands in the control group. The feature of this pattern has been demonstrated as follows:

Appearance of a new protein band of MW 195.36 kDa with absence of 3 bands of high

MW (168.21, 75.403 and 79.343). 3 new bands with MW 73.104, 57.4 and 45.704 kDa were clearly seen. 8 bands sized between 9.432 and 56.8 kDa disappeared in G<sub>1</sub> group, furthermore 5 visible bands ranged between 2.811 to 39.185 kDa were clearly seen in G<sub>1</sub> group and they were absent in the control group. Also, there were 3 bands with MW 24.806, 20.871 and 18.548 kDa found in the control and G<sub>1</sub> groups.

Electrophoretic protein pattern of the recovery group (G<sub>2</sub>) of newly born mice plasma:

Table (1) and figure (3) showed several changes in the relative percentages and total number of bands of plasma protein fractions of G<sub>2</sub> group as a result of disappearance of some original bands and appearance of other new ones which were different from that of the control group and exposed group.

The number of protein bands was approximately 17 bands which represented certain changes in the protein regions and they were demonstrated as follows:

In group G<sub>2</sub>, there were new 14 protein bands (MW ranged between 4.649 and 193.1 kDa), while 11 bands (MW ranged between 9.432 and 168.21 kDa) were present in the control group and absent in this group. Only 3 bands were present in both groups (Control and G<sub>2</sub> groups) at MW 40.667, 28.645 and 24.806 kDa.

## **Eye**

### **1- Histological results:**

Fig (4A) shows the three layers of the eye in normal contralateral newborn mice: sclera (Sc), choroid (Ch) and retina with its different sub layers, retinal pigmented epithelia (RPE), photoreceptor cells (rods and cones) with their outer (OS) and inner (IS) segments, outer limiting membrane (OLM), outer nuclear layer (ONL), outer plexiform layer (OPL), inner nuclear layer (INL), inner plexiform layer (IPL), ganglionic cell layer (GCL), nerve fiber layer (NFL) and inner limiting membrane (ILM).

Histological changes in the exposed group G<sub>1</sub> were shown in the form of degenerated and hemorrhagic areas of ganglionic cell layer, thinning of the inner nuclear layer, detachment in some areas of the outer nuclear layer and between inner and outer segments of the photoreceptors as well as retinal pigmented epithelial layer. Also, it was noted that there

were mild thickening of the nerve fiber layer, abnormal thickening in some areas of the choroid with increased melanin pigments, a wave like appearance of some retinal layers and absence of sclera in some areas (figure 4, B<sub>1,2&3</sub>). While in the recovery group G<sub>2</sub>, lesions were progressed to show separation predominantly in the inner and outer nuclear layers and between inner and outer segments of the photoreceptors (figure 4, C). Loss of most retinal pigmented epithelial cells and thinning of the choroid and sclera were also observed in G<sub>2</sub>.

By measurement of the mean thickness values in micrometer ( $\mu\text{m}$ )  $\pm$  standard deviation (SD) of the different layers of the eye in the experimental groups of newly born mice, it was demonstrated that there was a variation in the thickness of the different layers of the eye between the exposed, recovery and control groups as shown in table (2) and histogram (1), where inner plexiform layer, inner nuclear layer, photoreceptors and retinal pigmented epithelial thickness values were significantly reduced to reach  $13.72 \pm 0.28$ ,  $12.59 \pm 1.59$ ,  $12.27 \pm 0.73$  and  $0.93 \pm 0.07$  respectively in the exposed group G<sub>1</sub> and still reduced to reach  $11.28 \pm 1.28$ ,  $12.56 \pm 0.56$ ,  $12.62 \pm 0.88$  and  $0.98 \pm 0.18$  respectively in the recovery group G<sub>2</sub> in comparison with the control group in the same layers ( $14.24 \pm 0.24$ ,  $13.50 \pm 0.99$ ,  $14.44 \pm 0.56$  and  $2.21 \pm 0.29$  respectively). Conversely, the mean thickness values of the outer nuclear layer increased significantly to reach  $20.1 \pm 1.1$  and  $20.54 \pm 1.46$  in G<sub>1</sub> and G<sub>2</sub> respectively compared to the control group ( $16.01 \pm 0.51$ ). The mean thickness value of the layers: nerve fiber layer, ganglionic cell layer and outer plexiform layer were also significantly increased to reach  $7.42 \pm 1.42$ ,  $3.72 \pm 0.28$  and  $6.58 \pm 0.42$  respectively in group G<sub>1</sub> compared to the control group in these layers ( $4.1 \pm 0.50$ ,  $2.24 \pm 0.24$  and  $6.01 \pm 0.99$  respectively), but the mean thickness values of these layers were recovered and reduced to reach  $4.07 \pm 0.57$ ,  $1.85 \pm 0.05$  and  $2.82 \pm 0.32$  respectively in recovery group G<sub>2</sub>.

Table (2) and histogram (1) are also showing the mean thickness value of the choroid which was highly significantly increased ( $16.85 \pm 5.42$ ) in G<sub>1</sub> and highly reduced ( $1.89 \pm 0.19$ ) in G<sub>2</sub> in comparison with the control group ( $5.93 \pm 0.93$ ), while the mean thickness value in sclera showed

nearly no changes ( $3.55 \pm 0.55$ ) in  $G_1$  but highly significantly reduced ( $0.69 \pm 0.19$ ) in  $G_2$  compared to the control group ( $3.51 \pm 0.49$ ).

The mean thickness values of the different layers in eye of the experimental groups demonstrated the percentage similarity between them, since they reached 86.50% between the control and exposed group  $G_1$  and 85.02% between the control and recovery group  $G_2$  (Dendrogram 1). The choroid and sclera in the control eye of newly born mice were supported by bundles of collagen fibers which acquired blue color (figure 5, A), while the collagen deposition nearly disappeared in the exposed group  $G_1$  (figure 5, B) and reappeared in the choroid and sclera of the recovery group  $G_2$  (figure 5, C) as in the control group.

#### 2- Histochemical results:

Normal distribution of PAS + ve materials in eye layers of the control newly born mice with dense staining affinity in retinal pigmented epithelia, choroid and sclera (figure 6, A). Most eye layers of the exposed group  $G_1$  showed reduced stain affinity polysaccharides especially in the photoreceptors (figure 6, B), while PAS+ve materials were increased again in most layers of eye **of the recovery group  $G_2$  except in the choroid and sclera as revealed in figure (6, C).**

These results of PAS + ve materials in eye layers are in accordance with MOD values ( $\pm$ SD), where non significant decrease ( $1.48 \pm 0.12$ ) was detected in the exposed group  $G_1$  compared to the control group ( $1.58 \pm 0.11$ ) and raised to  $1.66 \pm 0.09$  in the recovery group  $G_2$  and it was higher than the control group as illustrated in table (3) and histogram (2).

In MOD values of PAS +ve materials in the eye, the percentage of similarity between the control and exposed group  $G_1$  was 94.75% and in case of the recovery group  $G_2$ , this percentage increased to 95.64% (Dendrogram 2).

Normal total protein was demonstrated in the eye layers of the control newly born mice with deeply stained choroid and sclera (figure 7, A). Increased proteinic content was realized in the eye layers of  $G_1$  and  $G_2$  groups (figure 7, B&C) with strong staining affinity in the exposed group  $G_1$  (figure 7, B).

These results of total protein of the eyes were supported by MOD values ( $\pm$ SD). The value of

MOD was  $1.46 \pm 0.42$  in the control group and significantly increased to  $1.64 \pm 0.57$  in  $G_1$ , while it went down again to  $1.53 \pm 0.52$  in  $G_2$  (Table 4 and histogram 3).

MOD values of total protein in the eyes indicated that the percentage similarity between the control and exposed group  $G_1$  was 77.96%, while this percentage between the control and recovery group  $G_2$  increased to 82.77% (Dendrogram 3).

figure (8, A) Demonstrated that there was a slight deposition of amyloid  $\beta$  in ganglionic cell layer, inner nuclear layer, outer nuclear layer, retinal pigmented epithelia, choroid and sclera in the normal control eye of newly born mice. Eyes of  $G_1$  and  $G_2$  groups (figure 8, B&C) showed increased accumulation of amyloid  $\beta$  materials in the retinal layers, choroid and sclera.

Increased amyloid  $\beta$  deposition in the eye was also detected by significantly increased MOD (Table, 5 and histogram 4). The MOD values ( $\pm$ SD) reached to  $1.71 \pm 0.61$  and  $1.86 \pm 0.48$  in  $G_1$  and  $G_2$  groups respectively compared to the control group ( $1.6 \pm 0.37$ ).

Dendrogram (4) showed the percentage of similarity of amyloid  $\beta$  MOD values in the eye between the experimental groups, since it was 95.23% between the control and exposed group  $G_1$  and it reached 89.14% in case of the recovery group  $G_2$ .

#### 3- Apoptosis and necrosis results:

The normal control eye of the newly born mice is showing a green vital regions in most layers as illustrated in figure (9, A).

In figure (9, B& C), the exposed ( $G_1$ ) and recovery ( $G_2$ ) groups showed late apoptotic cells and necrotic areas in the inner and outer nuclear layers which acquired orange chromatin in the nuclei that were highly condensed. Yellow early apoptotic cells of choroid were also noticed.

### Discussion

In the present study newly born mice were chosen as experimental animals and they were exposed to RF-EMF (900- 1800 MHz) emitted from mobile phone radiation, 45 min/day for one month.

#### Plasma proteins

In this experiment, SDS-PAGE electrophoresis technique was used to separate proteins and measuring the different types of these proteins.

The fractions which are containing the marker, reasonably well separated from other proteins, were subjected to SDS-PAGE. This marker consists of 8 proteins spanning the molecular weight range from 7 to 175 kDa. Each marker component is pre-stained covalently with a dye. According to the current study, it was possible to discriminate the structural changes induced by RF-EMF emitted mobile phone radiation. Digestion of protein chains by SDS resulted in 14 fractions of peptides (MW ranged from 168.21 to 9.432 kDa) for normal control newly born mice plasma which was separated by PAGE method. There were seven bands of proteins with high molecular weights and another seven bands with low molecular weights. 13 proteins of high MW were identified in the first six regions and the low MW proteins in the seventh region.  $\alpha_1$ -lipoprotein,  $\alpha_2$ macroglobulins and  $\gamma$ -globulins were demonstrated in region I and the iron-transport protein and transferrin were observed in region II, while the albumin, prealbumin, prothrombin and antithrombin were detected in region III.  $\alpha_1$ -antitrypsin and  $\beta_2$ -glycoprotein I were demonstrated in region IV and  $\alpha_1$ -acid glycoproteins,  $\beta_2$ -Glycoprotein III were observed in regions V, VI respectively.

The present results showed that the exposure of newly born mice to mobile phone radiation 45 min/day for one month (exposed group) as well as after one month following the end of exposure (recovery group) resulted in changes in the protein pattern. Since, the number of protein fractions in the exposed group decreased (12), but the recovery group recorded the largest numbers of the fractions (17) in comparison with the control group (14). This difference in the number of protein bands in the exposed and recovery groups was indicated by the appearance of new bands and disappearance of other ones. These results agree with the results of **Fragopoulou *et al.* [12]** which suggested that mobile phone radiation affect the protein pattern of hippocampus, cerebellum and frontal lobe of mice.

Region IV which represented  $\alpha_1$ -Antitrypsin and  $\beta_2$ -glycoprotein I had the highest concentration of all regions identified in the control and exposed group. While, the highest concentration of all regions identified in the recovery group

appeared in region V and represented  $\alpha_1$ -Acid glycoproteins.

The previous results indicated some alterations in plasma protein pattern of the exposed and recovery groups in comparison with the control group which may lead to functional disorders. This result agree with those of **Leszczynski *et al.* [29]**, who exposed human endothelial cells to 900 MHz RF radiation for 1 hour and observed alteration in number of proteins immediately after exposure.

**Nylund and Leszczynski [30]** observed that the mobile phone radiation (RF-EMF) induced statistically significant changes in the expression of several tens of proteins in human endothelial cell lines. Also, systematic protein analysis of the MCF-7 cells revealed that a few but different proteins were differentially expressed under continuous or intermittent RF-EMF exposure utilized in mobile phone for 24 h or less [31]. In addition, the mobile phone radiation might alter protein expression in human skin [10]. Their analysis has identified 8 proteins that were statistically significantly affected. Similarly, **Li [32]** also realized positive effects of EMF radiation exposure on protein expression profiles.

Moreover, **Seyyedi *et al.* [33]** studied the effect of EMF on human fibroblast, they used 3 Hz sinusoidal continuous EMFs, 3 hours duration and 4mT MF intensity and they showed that some protein patterns were affected by radiation after comparing the two-dimensions electrophoreses separated proteins from the exposed and control cells. The two proteins that their expression was reduced about 50% were determined as alpha 1 antitrypsin and transthyretin.

**Sulpizio *et al.* [34]** investigated the effects of 50 Hz, 1 mT sinusoidal EMF on protein expression of human neuroblastoma cells. Through comparative analysis between the exposed and control samples, they identified new nine proteins after 15- days of exposure. They suggested that the proteins were involved in a cellular defense mechanism and/or in cellular organization and proliferation.

This investigation confirmed the present results of an association between EMF and appearance of new bands of proteins. Although there were new 9 protein bands in the exposed group and

new 14 protein bands in the recovery group, while they were not found in the control group. However, there were 11 bands in the control group and absent in the exposed and recovery groups. In this respect, **Sharaf-Eldeen *et al.* [35]** found that the liver of rats exposed to mobile phone of 900 MHz for 14, 30, 45 days recorded an increase in number of fractions by 4 to 6 bands. The irradiated animals revealed 9 new synthesized proteins with different molecular weights. Also, **Ki-Bum *et al.* [36]** studied protein expression profile of breast cancer cells and they revealed that a few but different proteins were differentially expressed under RF radiation exposure. On the other hand, **French *et al.* [37]** proposed that repeated exposure to mobile phone radiation acts as a repetitive stress leading to continuous expression of stress protein in exposed cells and tissues as the heat shock proteins.

#### **Eye**

Eye is potentially susceptible to MF, since its limited blood supply means that it cannot easily dissipate heat. In addition, it does not have a bony protection that the brain receives from the skull. In particular, the retina is directly exposed to the electromagnetic radiation, so it is very sensitive due to the polar character of the photoreceptor cells as well as to its high water content [38]. It is well known that the retina is the source of ocular growth regulating signals and those retinal pigment epithelial cells are intimately involved in eye growth regulation [39]. All of these gave stimulation to examine the possible damage effect of mobile phone radiation on the different layers of the eye. Several studies have also demonstrated that there are relationship between electromagnetic radiation and retinal damage [15, 40].

The present study showed the normal histological structure of eye of the control newly born mice which showed three distinct layers: sclera, choroid and retina with its different sub layers, retinal pigmented epithelia, photoreceptor cells (rods and cones) with their outer and inner segments, outer limiting membrane, outer nuclear layer, outer plexiform layer, inner nuclear layer, inner plexiform layer, ganglionic cell layer, nerve fibers layer and inner limiting membrane.

Histopathological alterations in the mobile phone exposed group (45 min/day for one month) were detected in the form of degenerated and hemorrhagic areas of the ganglionic cell layer and mild thickening of the nerve fibers layer. Also, it was noted that there were, thinning of the inner nuclear layer, detachment in some areas of the outer nuclear layer and between inner and outer segments of the photoreceptors as well as retinal pigmented epithelial layer. In addition, there were abnormal thickening in some areas of the choroid with increased melanin pigments, a wave like appearance of some retinal layers and absence of sclera in some areas. Meanwhile in the recovery group, lesions were progressed to show predominant separation in the inner and outer nuclear layers and between inner and outer segments of the photoreceptors. Loss of most retinal pigmented epithelial cells and thinning of the choroid and sclera were also observed in this group.

These alterations agree with the data obtained by measurement of the mean thickness values (in  $\mu\text{m} \pm \text{SD}$ ) of the different layers of the eye in the experimental groups of newly born mice. It was demonstrated that there was a variation in the thickness of the different layers of the eye between the exposed, recovery and control groups, where inner plexiform layer, inner nuclear layer, photoreceptors and retinal pigmented epithelial thickness values were significantly reduced to reach  $13.72 \pm 0.28$ ,  $12.59 \pm 1.59$ ,  $12.27 \pm 0.73$  and  $0.93 \pm 0.07$  respectively in the exposed group and still reduced to reach  $11.28 \pm 1.28$ ,  $12.56 \pm 0.56$ ,  $12.62 \pm 0.88$  and  $0.98 \pm 0.18$  respectively in the recovery group in comparison with the control group in the same layers ( $14.24 \pm 0.24$ ,  $13.50 \pm 0.99$ ,  $14.44 \pm 0.56$  and  $2.21 \pm 0.29$  respectively). Controversially, the mean thickness values of the outer nuclear layer increased significantly to reach  $20.1 \pm 1.1$  and  $20.54 \pm 1.46$  in the exposed and recovery groups respectively compared to the control group ( $16.01 \pm 0.51$ ). The mean thickness values of the layers: nerve fibers layer, ganglionic cells layer and outer plexiform layer were also significantly increased to reach  $7.42 \pm 1.42$ ,  $3.72 \pm 0.28$  and  $6.58 \pm 0.42$  respectively in the exposed group compared to the control group in these layers

( $4.1\pm 0.50$ ,  $2.24\pm 0.24$  and  $6.01\pm 0.99$  respectively), but the mean thickness values of these layers were recovered and reduced to reach  $4.07\pm 0.57$ ,  $1.85\pm 0.05$  and  $2.82\pm 0.32$  respectively in the recovery group. Also, the mean thickness value of the choroid was highly significantly increased ( $16.85\pm 5.42$ ) in the exposed group and highly reduced ( $1.89\pm 0.19$ ) in the recovery group in comparison with the control group ( $5.93\pm 0.93$ ), however, the mean thickness value in the sclera showed nearly no changes ( $3.55\pm 0.55$ ) in the exposed group, but it was highly significantly reduced ( $0.69\pm 0.19$ ) in the recovery group compared to the control group ( $3.51\pm 0.49$ ). Therefore, the percentage similarity of the mean thickness values of the different layers of the eye between the experimental groups reached 86.50% between the control and exposed group and 85.02% between the control and recovery group. These findings were similar to the results reported by **Nassar *et al.* [18]** who investigated the adverse effects of 900- 1800 MHz pulsed radiation emitted from a mobile phone on the retina of the developing albino mice. They found that the non-ionizing radiation of the mobile phone has a marked degenerative effect on the retina of the exposed animals at the ultrastructural level. All the retinal layers exhibited an obvious reduction in their height and cell population. Besides, histological changes such as vacuolation and pale areas in the inner segment of photoreceptors, outer plexiform layer, inner nuclear layer and ganglionic cell layer were observed in the retina of albino rats which exposed 1 hrs daily for 4 weeks to mobile phone radiation [41].

Results of the present study are also supported by the results of **Khalil *et al.* [19]** who evaluated the possible toxicological effects of exposure to 900 MHz RF radiation emitted from a mobile phone on the histology and ultrastructure of retina of mice (30 min/day) for a month. They observed that RF radiation caused noticeable differences between photoreceptors of retina of the control and exposed groups as bleaching of photoreceptors of the exposed mice.

According to **Watson and Young [42]** the sclera is composed mainly of collagen fibrils which are mostly distributed among the equator and posterior pole region of

the eyeball. Thus, the current study demonstrated the bundles of collagen fibers in both of choroid and sclera in the control eye of newly born mice, while these bundles of collagen were nearly disappeared in the exposed group and reappeared in the recovery group. This observed result is in agreement with that of **Wang *et al.* [43]** who reported that the exposure to extremely low frequency EMFs resulted in a decreased proliferation rate of human fetal scleral fibroblasts and a significant decrease in collagen synthesis.

Concerning polysaccharides, most eye layers of the exposed group showed reduced staining affinity of polysaccharides especially in the photoreceptors, while PAS+ve materials were increased again in most layers of eye of the recovery group except in the choroid and sclera. These results of PAS + ve materials in the eye layers agree with MOD values ( $\pm$ SD), where non significant decrease ( $1.48\pm 0.12$ ) was detected in the exposed group compared to the control group ( $1.58\pm 0.11$ ) and raised to  $1.66\pm 0.09$  in the recovery group and it was higher than the control group. In PAS +ve materials of the eye, the percentage of similarity in MOD values was 94.75% between the control and exposed group and increased to 95.64% in case of the recovery group. Reduction of carbohydrate can be associated with multiple cerebellar eye signs including ocular flutter, and congenital ocular motor apraxia [44].

In the present study, increased proteinic content was realized in the eye layers of exposed and recovery groups with strong staining affinity in the exposed group. These results of total protein of the eyes were supported by MOD values ( $\pm$ SD). The value of MOD was  $1.46\pm 0.42$  in the control group and significantly increased to  $1.64\pm 0.57$  in the exposed group, while the value went down again to  $1.53\pm 0.52$  in the recovery group. In addition, MOD values of total protein in the eyes indicated that the percentage similarity between the control and exposed group was 77.96%, while this percentage increased to 82.77% between the control and recovery group. When the proteins of the eye lens increase, they begin to clump and scatter light to cause cataracts form. According to the world health organization, cataracts are the leading cause of vision impairment worldwide



[45]. According to Ali [46] there was an increase in the molecular weight of proteins in some regions of eye of rats after exposure to 50 Hz EMF.

Results of the present study revealed that eyes of the exposed and recovery groups showed increased accumulation of amyloid  $\beta$  materials in the retinal layers, choroid and sclera. The increase of amyloid  $\beta$  deposition in the eye was also detected by significantly increased MOD ( $\pm$ SD). Where, MOD values reached  $1.71\pm 0.61$  and  $1.86\pm 0.48$  in the exposed and recovery groups respectively compared to the control group ( $1.6\pm 0.37$ ). Thus, the percentage of similarity of amyloid  $\beta$  MOD values in the eye was 95.23% between the control and the exposed group and it reached 89.14% in case of the recovery group. This accumulation of amyloid  $\beta$  may contribute to 30% reduction of photoreceptors and the coating of amyloid  $\beta$  on outer segments may also have an impact upon visual function with age [47].

Concerning apoptosis, the exposed and recovery groups showed late apoptotic cells and necrotic areas in the inner and outer nuclear layers with highly condensed chromatin in their nuclei, besides, presence of apoptotic cells in the choroid. This increased incidence of apoptotic and necrotic neural cells in the inner and outer nuclear layer recorded in the present study come in agreement with those of Sasaki *et al.*, [48] and Nassar *et al.* [18]. According to Ozguner *et al.* [49] there was an increase in retinal levels of nitric oxide (an oxidant product) and malondialdehyde (an index of lipid peroxidation) which were used as markers of retinal oxidative stress in rats due to long-term exposure to 900 MHz EMR emitting mobile phones. This retinal oxidative stress may lead to apoptosis. The thermal effects of microwaves on the eye included cataracts, corneal edema, endothelial cell loss and retinal degeneration. Cell cycle abnormalities and early apoptosis were reported by Vignal *et al.* [50] due to the oxidative stress. Moreover, the study of Guler *et al.* [51] revealed the apoptotic cell formation in the eyes, using histopathological and immunohistochemical methods, in the non-pregnant and pregnant white rabbits and in offsprings of the pregnant group exposed to mobile phone radiation (1,800 MHz frequency).

**In conclusion**, Results of this study indicated that the exposure of newly born mice to RF-EMF emitted from mobile phone caused some alterations in plasma protein pattern which may lead to functional disorders. In addition, many histological and histochemical changes in the eye as well as increase of amyloidosis feature with apoptotic and necrotic effects in the eye. These effects were permanent after the end of exposure and there is no complete recovery from the damage produced by RF-EMF on the studied plasma protein and eye.

## References

1. Dimbylow PJ, Mann SM (1994): SAR calculations in an anatomically realistic model of the head for mobile communication transceivers at 900 MHz and 1.8 GHz. *Phys. Med. Bioll.*, 39:1537-1544.
2. Rothman KJ, Chou CK, Morgan R, Balzano Q, Guy AW, Funch DP (1996): Assessment of cellular telephone and other radio frequency exposure for epidemiologic research. *Epidemiology*, 7:291-298.
3. Bayazit V, Bayram B, Pala Z, Atan O (2010): Evaluation of carcinogenic effects of electromagnetic fields (EMF). *Bosn J. Basic Med. Sci.*, 10(3):245-250.
4. Kheifets L, Repacholi M, Saunders R, Deventer E (2005): The sensitivity of children to electromagnetic fields. *Pediatrics*, 116(2):303-313.
5. Kabuto M, Nitta H, Yamamoto S (2006): Childhood leukemia and magnetic fields in Japan: a case-control study of childhood leukemia and residential power-frequency magnetic fields in Japan. *Int. J. Cancer.*, 119:643-650.
6. Kolodynski AA, Kolodynska VV (1996): Motor and psychological functions of school children living in the area of the Skruna radio location station in Latvia. *Sci. Total Environ.*, 180:87-93.
7. Challis L (2005): RF interaction mechanisms. *Bioelectromagnetics*, 26(7):98-106.
8. Krstic DD, Ind IC, Sokolovic DT, Markovic VV, Petkovic DM, Radic SB (2005): The results of experimental exposition of mice by mobile telephones. In: *Microwave Review. T.E.L.S.I.K.S. Conference, Serbia and Montenegro*, pp: 34-37.
9. Lixia S, Yao K, Kaijun W, Deqiang L, Huajun H, Xiangwei G, Baohong W, Wei Z, Jianling L, Wei W (2006): Effects of 1.8

- GHz radiofrequency field on DNA damage and expression of heat shock protein 70 in human lens epithelial cells. *Mut. at Res.*, 602(1-2):135-142.
10. **Karinen A, Heinavaara S, Nylund R, Leszczynski D (2008):** Mobile phone radiation might alter protein expression in human skin. *Radiation and Nuclear Safety Authority B.M.C. Genomics*, 11:9-77.
  11. **Sypniewska RK, Millenbaugh NJ, Kiel JL, Blystone RV, Ringham HN, Mason PA, Witzmann FA (2010):** Protein Changes in Macrophages Induced by Plasma From Rats Exposed to 35 GHz Millimeter waves. *Bioelectromagnetics*, 31:656-663.
  12. **Fragopoulou AF, Samara A, Antonelou MH, Xanthopoulou A, Papadopoulou A, Vougas K, Koutsogiannopoulou E, Anastasiadou E, Stravopodis DJ, Tsangaris GTh, Margaritis LH (2012):** Brain proteome response following whole body exposure of mice to mobile phone or wireless DECT base radiation. *Electromagnetic Biology and Medicine*, 1:25-36.
  13. **Stang A, Anastassiou G, Ahrens W, Bromen K, Bornfeld N, Jockel KH (2001):** The possible role of radiofrequency radiation in the development of uveal melanoma. *Epidemiology*, 12: 7-12.
  14. **Balik HH, Turgut-Balik D, Balikci K, Özcan IC (2005):** Some ocular symptoms and sensations experienced by long term users of mobile phones. *Original Research Article Pathologie Biologie*, 53(2):88-91.
  15. **Balci M, Devrim E, Durak I (2007):** Effects of mobile phones on oxidant/antioxidant balance in cornea and lens of rats. *Curr. Eye Res.*, 32(1):21-25.
  16. **Kucer N (2008):** Some ocular symptoms experienced by users of mobile phones. *Electromagn. Biol. Med.*, 27(2):205-209.
  17. **Wu W, Yao K, Wang KJ, Lu DQ, He JL, Xu LH, Sun WJ (2008):** Blocking 1800 MHz mobile phone radiation-induced reactive oxygen species production and DNA damage in lens epithelial cells by noise magnetic fields. *Zhejiang Da Xue. Xue. Bao. Yi Xue. Ban.*, 37(1):34-38.
  18. **Nassar SA, Emam NM, Eid FA, Mohammed WT (2011):** Effects of non-ionizing radiation on the ultrastructure of the retina of albino mice. *J. of American Science*, 7(12):1196-1208.
  19. **Khalil A, Al-Adhammi M, Al-shara B, Gagaa M, Rawshdeh A, Alshamli A (2012):** Histological and ultrastructural analyses of male mice exposed to mobile phone radiation. *J. of Toxicology Review*, 1(1): 1-6.
  20. **Bancroft JD, Gamble M (2002):** *Theory and Practice of Histological Techniques*. 5<sup>th</sup> ed., Churchill livingstone. London. pp: 150-152.
  21. **Pearse AG (1977):** *Histochemistry, Theoretical and Applied*. 3<sup>rd</sup> ed., Livingstone, C., London. p.1.
  22. **Hotchkiss RD (1948):** A microchemical reaction resulting in the staining of polysaccharide structures in fixed tissue preparations. *Arch. Biochem.*, 16: 131-132.
  23. **Mazia D, Brewer PA, Alfert M (1953):** The cytochemical staining and measurement of protein with mercuric bromophenol blue. *Biol. Bull.*, 104:57-67.
  24. **Sheehan DC, Hrapchak BB (1980):** *Theory and Practice of Histochemistry*. 2<sup>nd</sup> ed., Mosby, St. Louis (MO), London, pp: 177-178.
  25. **Valle S (1986):** Special stains in microwave oven. *J. Histotechnol.*, 9:237-248.
  26. **Ribble D, Goldstein NB, Norris DA, Shellman YG (2005):** A simple technique for quantifying apoptosis in 96-well plates. *B.M.C. Biotechnol.*, 10:5-12.
  27. **Reedy CL, Kamboj S (2004):** *Image Analysis Protocol Instructions #1: Spatial Calibration of Images, using image-pro plus*. Clemex Vision P.E. and image J., University of Delaware, Laboratory for Analysis of Cultural Materials.
  28. **Clarke KR, Gorley RN (2001):** *Primer Version 5*. Primer- E, Plymouth, UK.
  29. **Leszczynski D, Joenvaara S, Reivinen J, Kuokka R (2002):** Non-thermal activation of the hsp27/p38MAPK stress pathway by mobile phone radiation in human endothelial cells: molecular mechanism for cancer- and blood-brain barrier-related effects. *Differentiation*, 70:120-129.
  30. **Nylund R, Leszczynski D (2004):** Proteomics analysis of human endothelial cell line EA.hy926 after exposure to GSM 900 radiation. *Proteomics*, 4:1359-1365.
  31. **Zeng Q (2006):** Effects of global system for mobile communications 1800 MHz radiofrequency electromagnetic fields on gene and protein expression in MCF-7 cells. *Proteomics*, 6:4732-4738.
  32. **Li H (2005):** Effects of ELF magnetic fields on protein expression profile of human breast cancer cell MCF7. *Sci. China C. Life Sci.*, 48: 506-514.
  33. **Seyyedi SS, Dadras MS, Tavirani MR, Mozdarani H, Toossi P, Zali AR (2007):** Proteomic analysis in human fibroblasts by continuous exposure to extremely low-frequency electromagnetic fields. *Pak. J. Biol. Sci.*, 10(22):4108-4112.

34. **Sulpizio M, Falone S, Amicarelli F, Marchisio M, Di Giuseppe F, Eleuterio E (2011):** Molecular basis underlying the biological effects elicited by extremely low-frequency magnetic field (ELF-MF) on neuroblastoma cells. *J. Cell Biochem.*, 112(12):3797-3806.
35. **Sharaf-Eldeen KhM, Zowail MEM, Abdel-Kareim AM (2005):** The protective effect of garlic on changes in liver and brain proteins occurring in albino rats exposed to 900 MHz (GSM) microwaves. *Medical J.*, (3):1-14.
36. **Ki-Bum KIM, Hae-Ok BYUN, Na-Kyung HAN, Young-Gyu KO, Hyung-Do CHO, Nam KIM, Jeong-Ki PACK, Jae-Seon LEE (2010):** Two-dimensional electrophoretic analysis of radio frequency radiation-exposed MCF7 breast cancer cells. *J. Radiat. Res.*, 51: 205-213.
37. **French PW, Penny R, Laurence JA, McKenzie DR (2001):** Mobile phones, heat shock proteins and cancer. *Differentiation*, 67(4-5): 93-97.
38. **Kovacs E, Savopol T, Dinu A (1995):** The polar behavior of frog photoreceptors. *Biochim. Biophys.*, 1273: 217-222.
39. **Rymer J, Wildsoet CF (2005):** The role of the retinal pigment epithelium in eye growth regulation and myopia: A review. *Vis. Neurosci.*, 22:251-261.
40. **Youssef PN, Sheibani N, Albert DM (2011):** Retinal light toxicity. *Eye (Lond.)*, 25(1): 1-14.
41. **Hanafy LK, Karam SH, Mansour SM (2012):** The possible adverse effect of mobile phone on the retina. *J. of Medicine and Medical Sciences*, 7(1): 38-43.
42. **Watson PG, Young RD (2004):** Scleral structure, organisation and disease: A review. *Exp. Eye Res.*, 78:609-623.
43. **Wang J, Cui J, Zhu H (2013):** Suppression of type I collagen in human scleral fibroblasts treated with extremely low-frequency electromagnetic fields. *Molecular Vision*, 19:885-893.
44. **Stark KL, Gibson JB, Hertle RW, Brodsky MC (2000):** Ocular motor signs in an infant with carbohydrate-deficient glycoprotein syndrome type Ia. *American J. of Ophthalmology*, 130(4): 533-535.
45. **McCarty CA, Nanjan MB, Taylor HR (2000):** Attributable risk estimates for cataract to prioritize medical and public health action. *Invest. Ophthalmol. Vis. Sci.*, 41: 3720-3725.
46. **Ali EM (2010):** Molecular changes observed in aqueous humour of eye following exposure to electromagnetic field. *Biophysics Unit, Research Institute of Ophthalmology, Giza, Egypt*.
47. **Kam JH, Lenassi E, Jeffery G (2010):** Viewing ageing eyes: diverse sites of amyloid beta accumulation in the ageing mouse retina and the up-regulation of macrophages. *Academic J.*, 5 (10):1-12.
48. **Sasaki K, Ino H, Chiba T, Adachi-Usami E (1999):** Light-induced apoptosis in the neonatal mouse retina and superior colliculus. *Invest. Ophthalmol. Vis. Sci.*, 40: 3079-3083.
49. **Ozguner F, Bardak Y, Comlekci S (2006):** Protective effects of melatonin and caffeic acid phenethyl ester against retinal oxidative stress in long term use of mobile phone: a comparative study. *Mol. Cell Biochem.*, 282(1-2): 83-88.
50. **Vignal R, Crouzier D, Dabouis V, Debouzy JC (2009):** Effects of mobile phones and radar radiofrequencies on the eye. *Pathol. Biol. (Paris)*, 57(6):503-508.
51. **Guler G, Ozgur E, Keles H, Tomruk A, Vural SA, Seyhan N (2011):** Apoptosis resulted from radiofrequency radiation exposure of pregnant rabbits and their infants. *Bull. Vet. Inst. Pulawy*, 55:127-134.

**Table (1).** The relative percentages of plasma protein fractions of newly born mice separated electrophoretically from the different experimental groups.

Region	Protein fraction	Estimated molecular weight (kDa)	Relative fraction percentages of the experimental groups		
			Control	Exposed	Recovery
I	$\alpha_1$ -Lipoprotein, $\alpha_2$ -macroglobulins and $\gamma$ -globulins	195.36	0	17.089	0
		193.1	0	0	16.211
		168.21	9.102	0	0
		165.95	0	0	6.457
II	Transferrin	79.343	0.455	0	0
		75.403	0.978	0	0
		74.09	0	0	7.239
III	Albumin prealbumin, prothrombin and Antithrombin	73.104	0	2.187	0
		59.97	0	0	4.848
		57.4	0	5.449	0
		56.8	8.222	0	0
		54.1	0	0	9.169
IV	$\alpha_1$ -Antitrypsin and $\beta_2$ -glycoprotein I	45.704	0	37.562	0
		44.815	50.760	0	0
V	$\alpha_1$ -Acid glycoproteins	43.333	0	0	21.864
		40.667	11.868	0	3.444
VI	$\beta_2$ -Glycoprotein III	39.185	0	13.217	1.948
		36.519	5.253	0	0
		34.148	0	2.687	0
VII	Low molecular weight proteins	32.963	0	0	6.701
		30.593	3.348	0	0
		29.435	0	4.765	0.877
		28.645	1.784	0	2.048
		27.629	0	4.006	0
		24.806	2.440	1.687	2.747
		23.565	0	0	0.212
		20.871	1.906	2.936	0
		18.935	0	0	11.889
		18.548	2.250	1.064	0
		12.946	1.229	0	0
		9.432	0.405	0	0
		8.892	0	0	0.128
		4.649	0	0	1.843
2.811	0	7.350	2.374		
<b>Number of fractions</b>			<b>14</b>	<b>12</b>	<b>17</b>

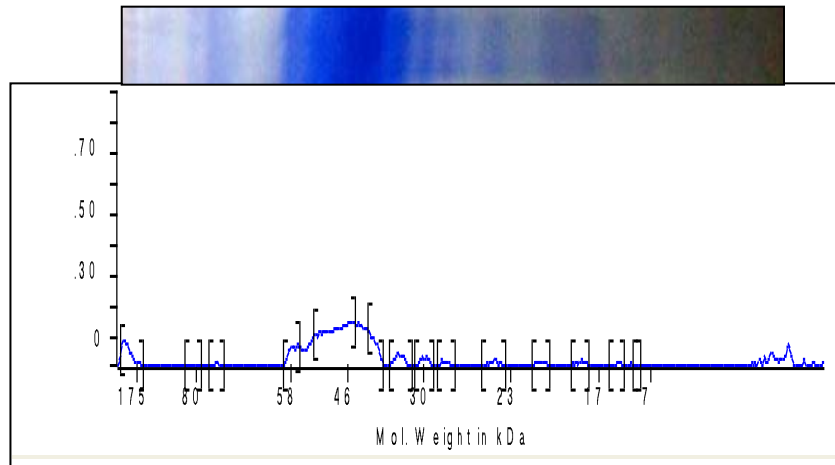


**Fig. (1).** Electropherogram of SDS- PAGE gel of the most common pattern of plasma proteins in the control newly born mice.

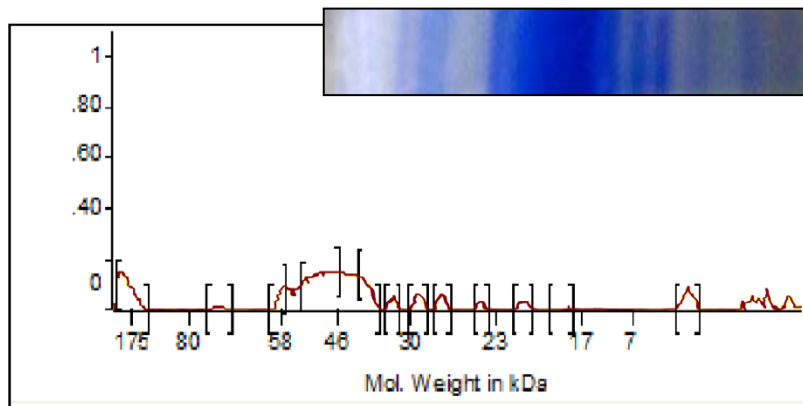


**Fig. (2).** Electropherogram of SDS- PAGE gel of the most common pattern of plasma proteins in newly born mice of the exposed group (G<sub>1</sub>).

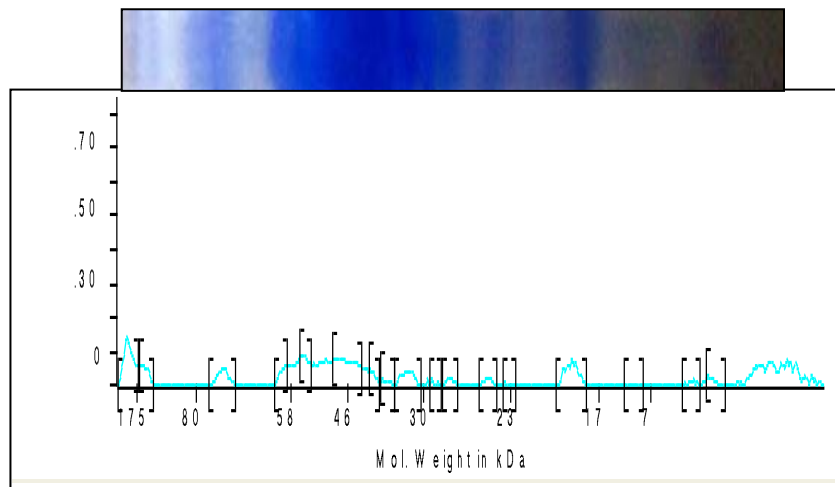


**Fig. (3).** Electropherogram of SDS- PAGE gel of the most common pattern of plasma proteins in newly born mice of the recovery group (G<sub>2</sub>).

Fig. (4)

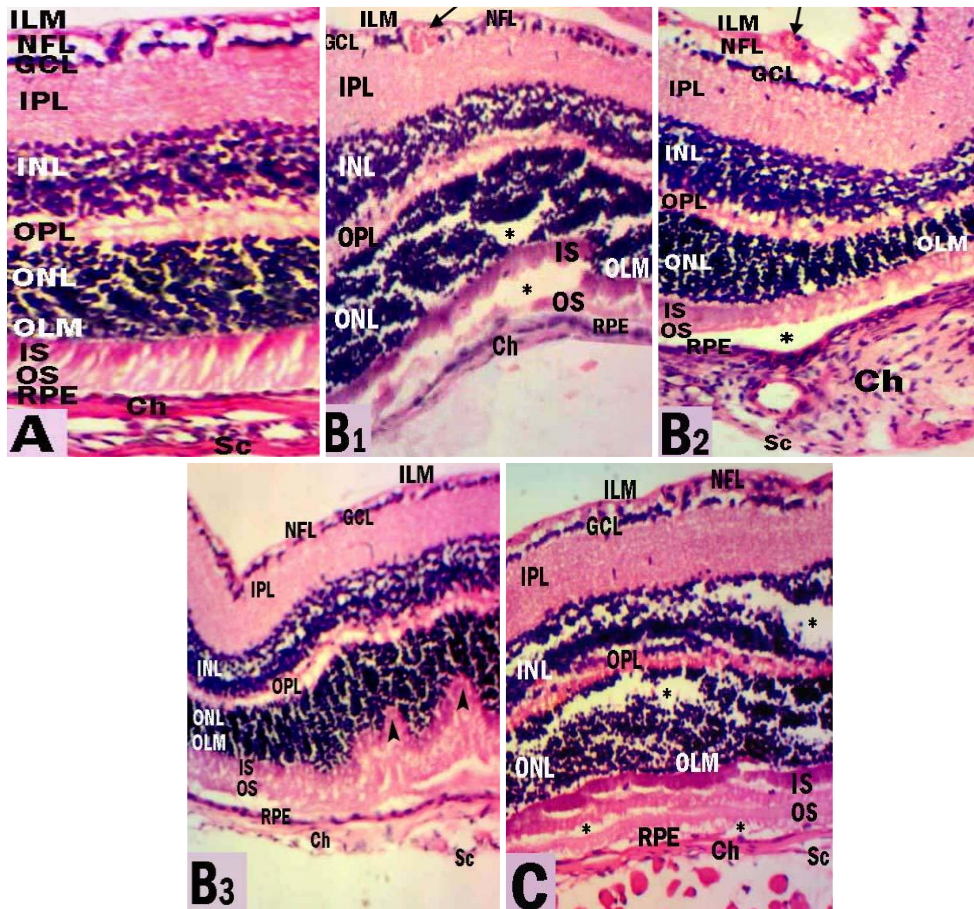


**Fig. (4).** Sections in eyes of newly born mice of the different groups:

A. Section in the control group showing the three layers of eye: sclera (Sc), choroid (Ch) and retina with its different sub layers, retinal pigmented epithelia (RPE), outer segment (OS) & inner segment (IS) of photoreceptor cells, outer limiting membrane (OLM), outer nuclear layer (ONL), outer plexiform layer (OPL), inner nuclear layer (INL), inner plexiform layer (IPL), ganglionic cell layer (GCL), nerve fiber layer (NFL) and inner limiting membrane (ILM).

B<sub>1,2,3</sub>. Sections in the exposed group G<sub>1</sub> showing:

B<sub>1</sub>. Degeneration of some areas of ganglionic cell layer with intraretinal hemorrhage (↓), thinning of the inner nuclear layer, detachment in some areas of the outer nuclear layer and between inner and outer segments of the photoreceptors (\*). Notice a complete absence of sclera in this area.

B<sub>2</sub>. Thickening of the nerve fiber layer (NFL) with hemorrhage in this layer (↓), detachment between the photoreceptors and retinal pigmented epithelia (\*) and abnormal thickening of the choroid with increased melanin pigments.

B<sub>3</sub>: wavelike appearance of some retinal layers (▲).

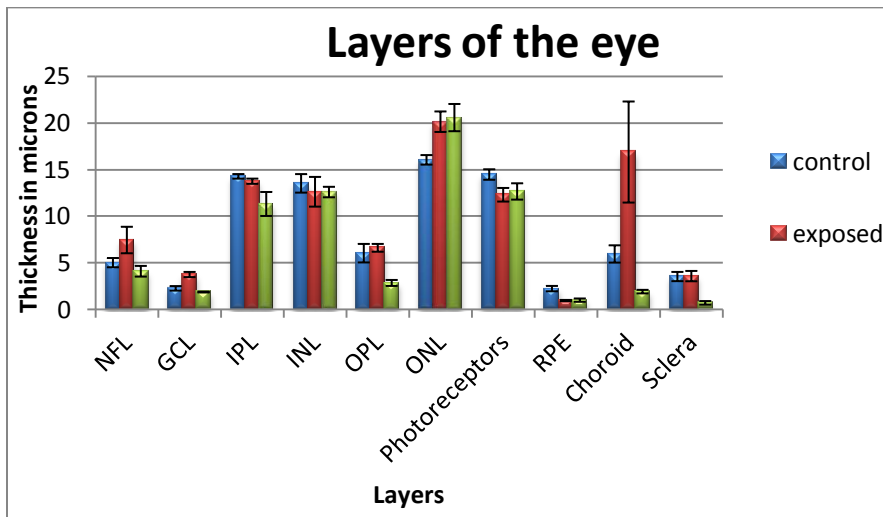
C. Section in the recovery group G<sub>2</sub> showing predominant separation in the inner and outer nuclear layers and between inner and outer segments of the photoreceptors (\*). Notice loss of most retinal pigmented epithelial cells and thinning of the choroid and sclera.

(Hx& E x 400)

**Table (2).** Thickness of the different layers of the eye of newlyborn mice in the different experimental groups.

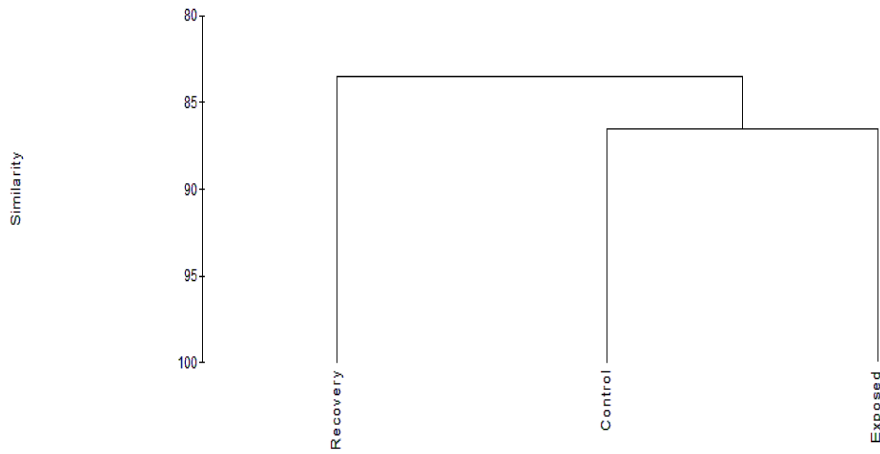
Layers of eye (µm)	Experimental groups		
	Control	Exposed	Recovery
NFL	4.1 ±0.50	7.42 ±1.42	4.07 ±0.57
GCL	2.24 ±0.24	3.72 ±0.28	1.85 ±0.05
IPL	14.24 ±0.24	13.72 ±0.28	11.28 ±1.28
INL	13.50 ±0.99	12.59 ±1.59	12.56 ±0.56
OPL	6.01 ±0.99	6.58 ±0.42	2.82 ±0.32
ONL	16.01 ±0.51	20.1 ±1.1	20.54 ±1.46
Photoreceptors	14.44 ±0.56	12.27 ±0.73	12.62 ±0.88
RPE	2.21 ±0.29	0.93 ±0.07	0.98 ±0.18
Choroid	5.93 ±0.93	16.85 ±5.42	1.89 ±0.19
Sclera	3.51 ±0.49	3.55 ±0.55	0.69 ±0.19

Data expressed as a mean of 5 records ± SD



**Histogram (1).** Average thickness (±SD) of the different layers of the eye of newly born mice in the different experimental groups.





**Dendrogram (1).** The similarity between the different experimental groups based on the thickness of the different layers of the eye.

**Fig. (5)**

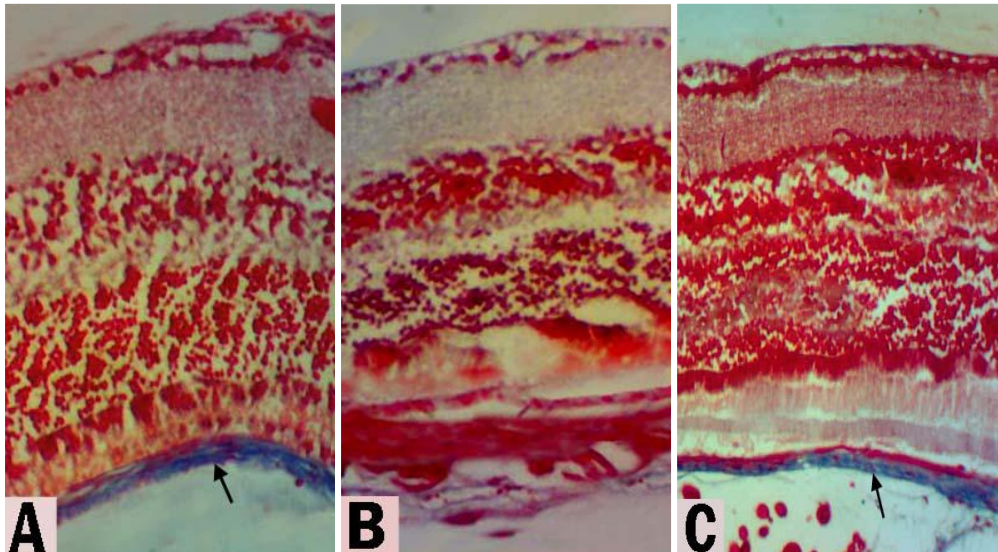


**Fig. (5).** Sections in eyes of newly born mice showing distribution of collagen fibers:  
A. Control group showing bundles of blue collagen fibers supporting the choroid and sclera (↑).  
B. Section in the exposed group G<sub>1</sub> showing nearly disappearance of collagen deposition.  
C. Section in the recovery group G<sub>2</sub> showing reappearance of collagen fibers in the choroid and sclera (↑).  
(Mallory's trichrome stain, x 400)



**Fig. (6)**

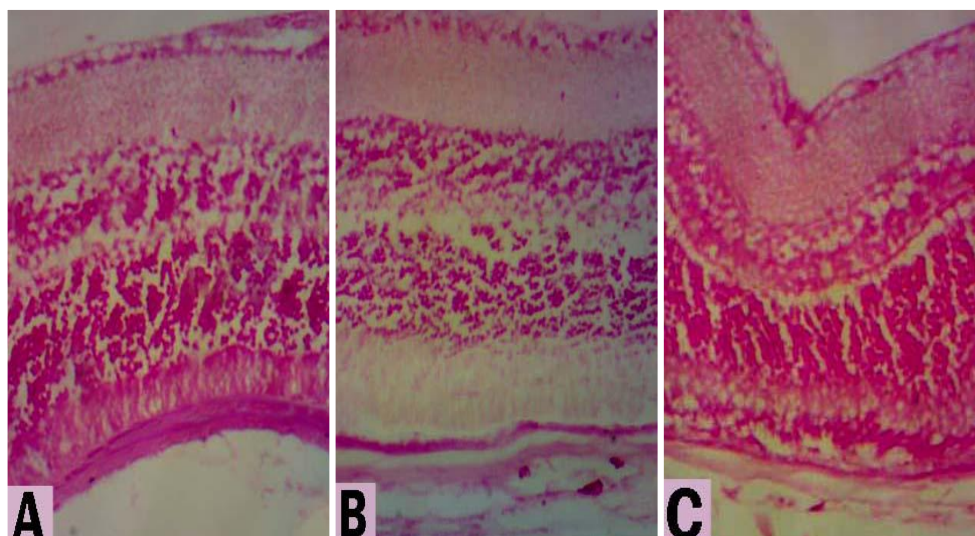
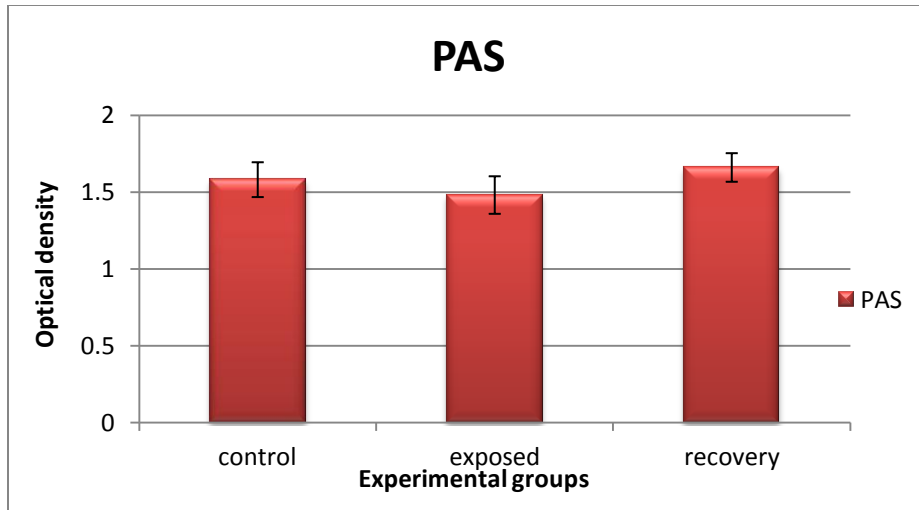


**Fig. (6).** Sections in eyes of newly born mice representing distribution of polysaccharides:  
 A. Section in the control group showing normal distribution of PAS+ve materials in eye layers with high stain affinity in retinal pigmented epithelia, choroid and sclera.  
 B. Section in the exposed group G<sub>1</sub> showing reduced PAS+ve materials in most layers and poorly stained photoreceptors.  
 C. Section in the recovery group G<sub>2</sub> showing increased PAS+ve materials in most layers of the eye except the choroid and sclera.  
 (PAS stain, x400)

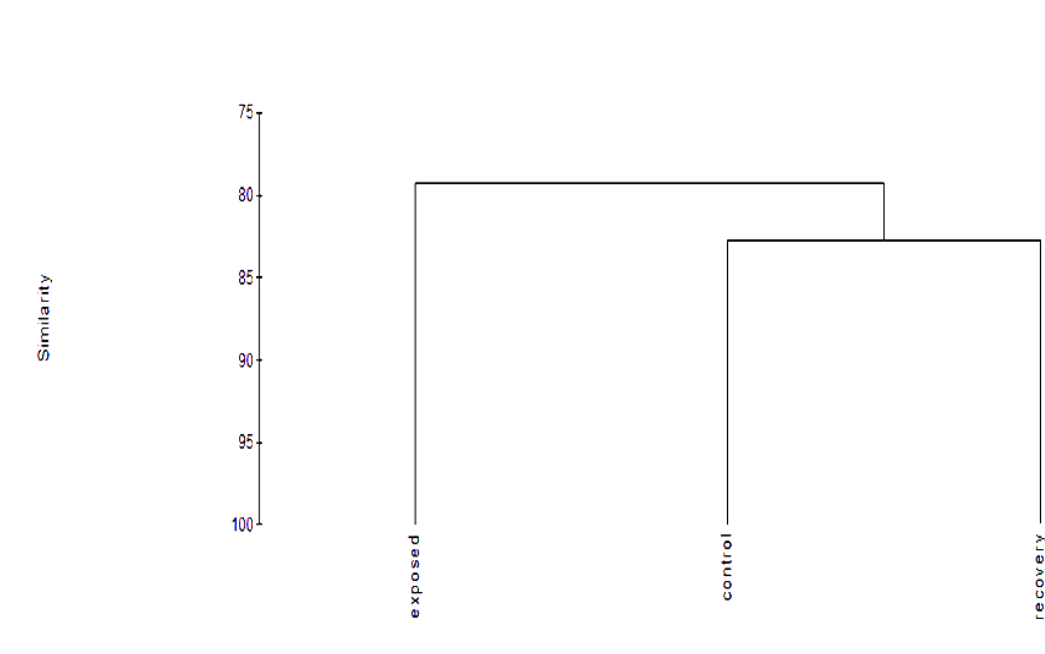
**Table (3).** The optical density values of PAS +ve materials in eye of newly born mice of the different experimental groups.

Organ	Experimental groups		
	Control	Exposed	Recovery
Eye			
PAS mean ±SD	1.58±0.11	1.48±0.12	1.66±0.09
PAS max	1.91	1.91	1.94
PAS mini	1.2	0.96	1.39

(Data expressed as a mean ± SD, maximum and minimum)



**Histogram (2).** The optical density values (mean±SD) of PAS +ve materials in eye of newly born mice of the different experimental groups.



**Dendrogram (2).** The similarity between the different experimental groups based on the optical density of PAS +ve materials in the eye.

**Fig. (7)**

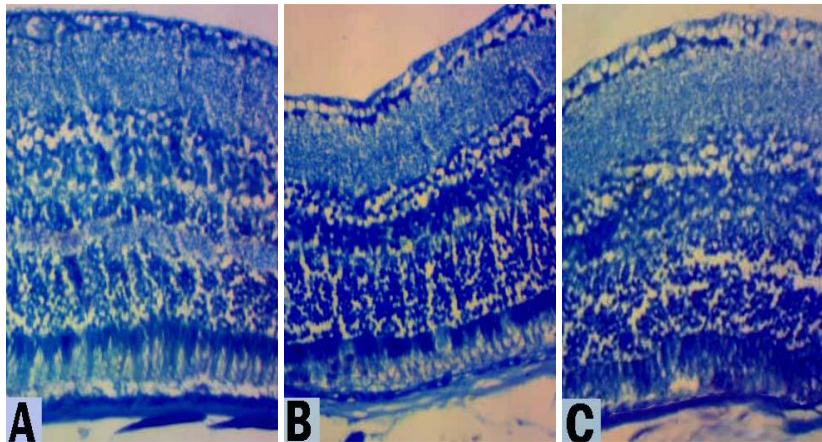
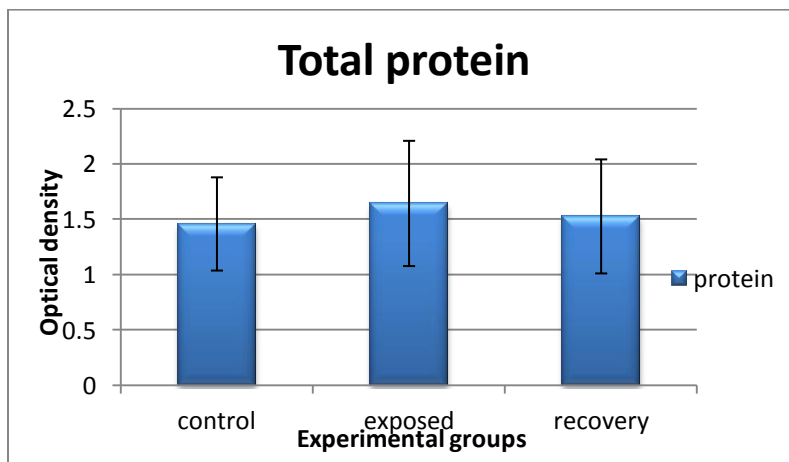


**Fig. (7).** Sections in eyes of newly born mice showing distribution of total protein:  
 A. Section in the control group showing normal distribution of total protein in layers of the eye with deeply stained choroid and sclera.  
 B & C. Sections in G<sub>1</sub>& G<sub>2</sub> groups showing a slight increase in their proteinic content and strong stain affinity in eye layers of the exposed group G<sub>1</sub> (B).  
 (Mercuric bromophenol blue stain x400)

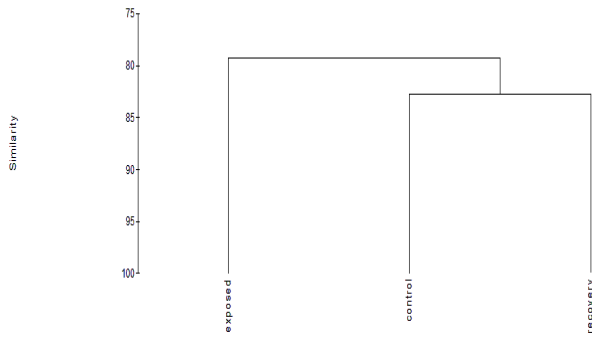
**Table (4).** The optical density values of total protein in eye of newly born mice of the different experimental groups.

Organ	Experimental groups		
Eye	Control	Exposed	Recovery
Total protein mean $\pm$ SD	1.46 $\pm$ 0.42	1.64 $\pm$ 0.57	1.53 $\pm$ 0.52
Total protein max	2.55	2.55	2.55
Total protein mini	0.16	0	0

(Data expressed as a mean  $\pm$  SD, maximum and minimum)



**Histogram (3).** The optical density values (mean $\pm$ SD) of total protein in eye of newly born mice of the different experimental groups.



**Dendrogram (3).** The similarity between the different experimental groups based on the optical density of total protein in the eye.

**Fig. (8)**

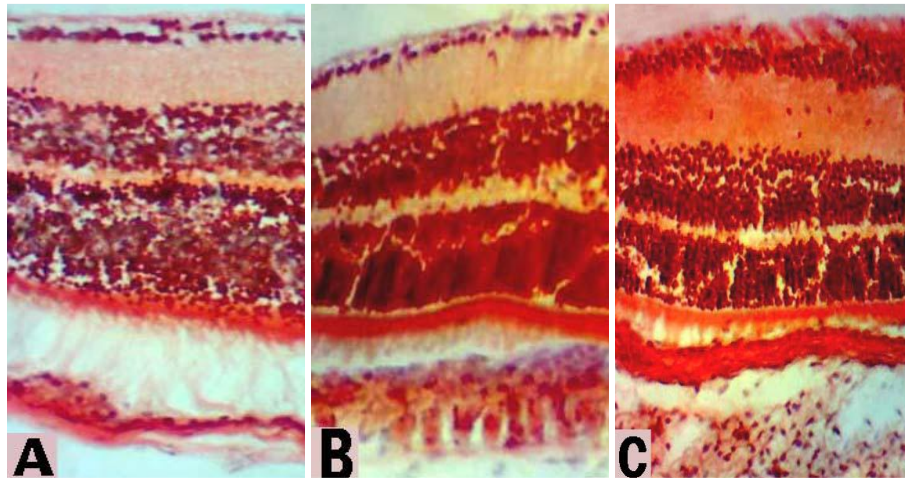


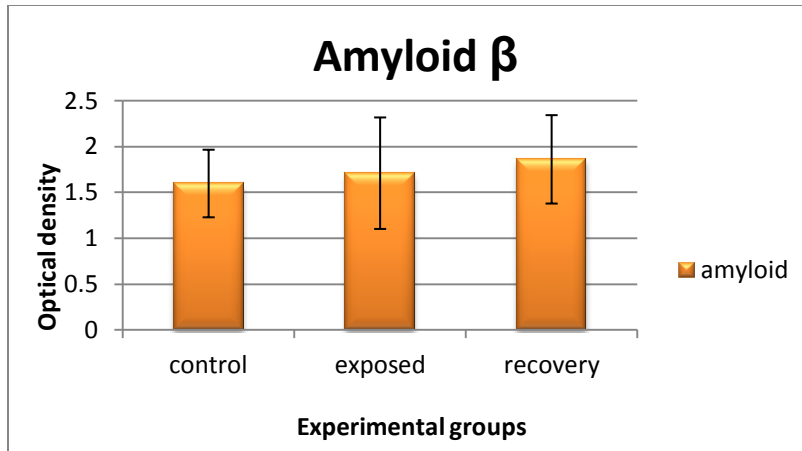
**Fig. (8).** Sections in eyes of newly born mice of the different groups showing distribution of amyloid  $\beta$ : A. Control group showing a slight deposition of amyloid  $\beta$  in GCL, INL, ONL, RPE, choroid and sclera. B&C. Sections in  $G_1$  &  $G_2$  groups showing increased accumulation of amyloid  $\beta$  material in the retinal layers, choroid and sclera.

(Congo red stain x400)

**Table (5).** The optical density values of amyloid  $\beta$  in eye of newly born mice of the different experimental groups.

Organ	Experimental groups		
Eye	Control	Exposed	Recovery
Amyloid $\beta$ mean $\pm$ SD	1.6 $\pm$ 0.37	1.71 $\pm$ 0.61	1.86 $\pm$ 0.48
Amyloid $\beta$ max	2.15	2.55	2.55
Amyloid $\beta$ mini	0.59	0.33	0.36

(Data expressed as a mean  $\pm$  SD, maximum and minimum)



**Histogram (4).** The optical density values (mean±SD) of Amyloid β in eye of newly born mice of the different experimental groups.



**Dendrogram (4).** Represents the similarity between the different experimental groups based on the optical density of Amyloid β in the eye.

**Fig. (9)**

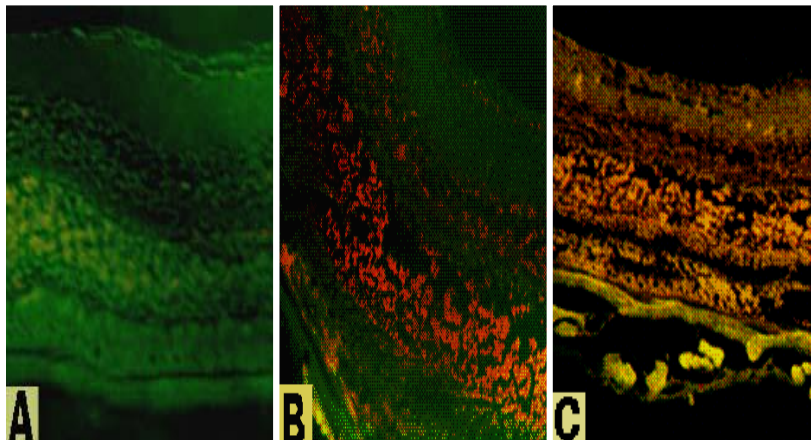


**Fig. (9).** Sections in eyes of newly born mice showing the apoptotic cells and necrotic areas:  
 A. Section in the control group showing vital regions in most layers of the eye.  
 B&C. Sections in G<sub>1</sub> & G<sub>2</sub> groups showing late apoptotic cells and necrotic areas in the inner and outer nuclear layers with orange chromatin in the nuclei and yellow early apoptotic cells in the choroid.  
 (Acridine orange/ethidium bromide stain x 400)